

Electronimpact excitation of autoionizing states in xenon

Deepak Mathur and David C. Frost

Citation: *The Journal of Chemical Physics* **75**, 5381 (1981); doi: 10.1063/1.441983

View online: <http://dx.doi.org/10.1063/1.441983>

View Table of Contents: <http://scitation.aip.org/content/aip/journal/jcp/75/11?ver=pdfcov>

Published by the [AIP Publishing](#)

Articles you may be interested in

[Polarization and correlations in electron-impact autoionization studies](#)

AIP Conf. Proc. **500**, 319 (2000); 10.1063/1.1302665

[Variable angle electronimpact excitation of nitromethane](#)

J. Chem. Phys. **72**, 2788 (1980); 10.1063/1.439427

[Electronimpact excitation of the lowlying electronic states of HCN](#)

J. Chem. Phys. **67**, 4835 (1977); 10.1063/1.434688

[Electronimpact excitation of the lowlying electronic states of formaldehyde](#)

J. Chem. Phys. **61**, 4279 (1974); 10.1063/1.1681731

[ElectronImpact Excitation of Nitric Oxide](#)

J. Chem. Phys. **56**, 2870 (1972); 10.1063/1.1677620



Electron-impact excitation of autoionizing states in xenon

Deepak Mathur^{a)} and David C. Frost^{b)}

Christopher Ingold Laboratory, University College London, 20 Gordon Street, London WC1H 0AJ, United Kingdom

(Received 26 May 1981; accepted 29 June 1981)

High-sensitivity single-ionization efficiency functions of Xe have been measured using a computer-controlled beam of electrons monoenergetic to ~ 45 meV FWHM. Well-defined structure detected in the energy range 12.2–13.5 eV is attributed to the excitation of neutral Xe Rydberg states converging on $\text{Xe}^+(^2P_{1/2})$ followed by autoionization. Some of the structure appears to correspond to parity forbidden $s-p'$ transitions. A sharp increase in ionization is observed at the $^2P_{1/2}$ threshold.

INTRODUCTION

A number of experiments have been conducted in recent years to study electron and photon induced excitation of Rydberg states of xenon below the $^2P_{1/2}$ limit.^{1–7} With the ground state having a configuration $np^6(^1S_0)$, excited states of the type np^5, ml can converge on either the $^2P_{3/2}$ or the $^2P_{1/2}$ ionization limits. Highly excited Rydberg states converging on the latter can therefore lie above the first ionization potential. Their degeneracy with the $^2P_{3/2}$ continuum can lead to autoionization expected to produce structure in the total ionization efficiency (IE) function between the $^2P_{3/2}$ and $^2P_{1/2}$ thresholds.

Mainly in the 1950's, many attempts to resolve fine structure in electron-impact IE functions unfortunately only produced a vast accumulation of mainly contradictory data (Ref. 8 and references therein). Recently, modern technology has facilitated the development of experiments using directly produced beams of nearly monoenergetic electrons to study IE functions with significantly improved resolution and signal-to-noise (S/N) ratios. The pioneering work of Marmet,⁵ Lossing,⁹ and co-workers and the more recent experiments of Johnson *et al.*¹⁰ and Suzuki and Maeda²¹ must be noted in this connection. Nevertheless, the published fine structure has sometimes^{5,13} emerged from a not inconsiderable degree of mathematical treatment of the experimental data.

We report here results of high sensitivity/stability measurements of the IE function for Xe^+ using a computer-controlled source of electrons monoenergetic to ~ 45 meV full width at half maximum (FWHM) and a quadrupole mass spectrometer. We have chosen Xe for two reasons: first, the position of Rydberg states lying between the $\text{Xe}^+ ^2P_{3/2}$ and $^2P_{1/2}$ limits are known to high precision^{1,3,4,7} and, second, two recent high resolution electron impact ionization studies^{5,10} are in contradiction to each other and differ also with IE functions for Xe^+ obtained using the more indirect methods of Grasso⁸ and Hashizume and Wasada.²

EXPERIMENTAL

The apparatus used is based on the original design of Maeda, Semeluk, and Lossing and the modifications have been described elsewhere.^{10–12} Briefly, two hemispherical electrostatic analyzers in tandem produce an electron beam of intensity $\sim 10^{-8}$ A and FWHM ~ 45 meV (as determined by scanning one analyzer against the other) which intersects an atomic beam at right angles in a room-temperature interaction zone enclosed by 92% transparent molybdenum mesh. The gas pressure in the interaction region is $\leq 10^{-5}$ Torr and the background pressure is $\leq 10^{-7}$ Torr. Ions formed are extracted into a quadrupole mass spectrometer by an extremely weak electric field at 90° to the incident electron beam and subsequently detected by an off-axis channel electron multiplier operating in the single particle counting mode. The acquisition of ion counts as a function of electron impact energy is controlled online by a PDP 8 mini-computer.

Subsidiary experiments¹¹ have shown the electron energy scale to be linear and to drift by much less than 20 meV over the usual 20 h data accumulation period used in the present measurements. The energy scale is calibrated with reference to the initial onset of Xe^+ production, taken to occur at 12.13 eV.⁸ The number of ion counts recorded per second in these measurements is typically ~ 1000 at an electron energy of 12.5 eV. An idea of the S/N ratio can be obtained by referring to Fig. 1.

RESULTS

Figure 1 shows a typical untreated IE function for Xe^+ produced by repetitively scanning the electron energy from 12.1 to 13.6 eV over about 20 h. Structure is easily discernible in the raw IE function and, of course, more so in its first differential. In order to improve the S/N ratio in the differential, some elementary data treatment was done, the results of which are shown in Fig. 2.

The top two curves of Fig. 2 result from simple moving averages (MA) smoothing using the method of fourth differences¹⁴ in which data smoothed once (1y_i) are given for a five-point smoothing algorithm by

$$(^1y_i) = \frac{1}{5} (y_{i-2} + y_{i-1} + y_i + y_{i+1} + y_{i+2}),$$

where $i = 3-1022$ for a set of 1024 raw data points. Fig-

^{a)} Now at Department of Physics, Birkbeck College, University of London, Malet Street, London WC1E 7HX, U.K. and Tata Institute of Fundamental Research, Homi Bhabha Road, Bombay 400 005, India.

^{b)} J. S. Guggenheim Memorial Fellow. Permanent address: Department of Chemistry, University of British Columbia, Vancouver VGT 1Y6, B.C., Canada.

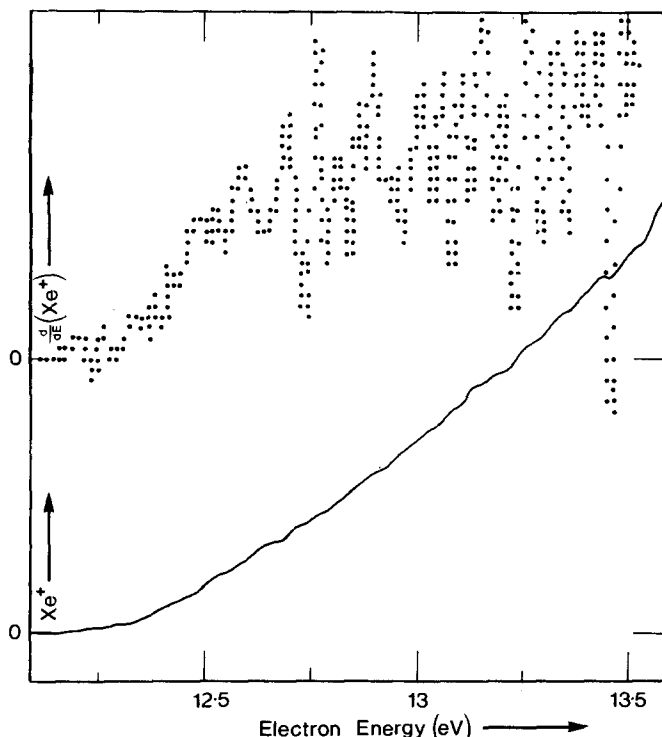


FIG. 1. The raw ionization efficiency function of xenon and its first differential obtained with an electron beam energy resolution ≈ 0.045 eV FWHM.

ure 2 shows that carrying out an increasing number of MA runs (represented by NSMTK) gives more "effective" smoothing at the expense of resolution. Despite this, there are strong basic similarities between the curves obtained after 30 and 100 smoothing treatments (see top two frames of Fig. 2).

We have also introduced a modification to the five-point smoothing algorithm by giving each of the five data points different weights whereby data that have been smoothed once are now given by

$$({}^1y_{iw}) = \frac{1}{35} [17y_i + 12(y_{i-1} + y_{i+1}) - 3(y_{i-2} + y_{i+2})].$$

The structure in the resulting data functions, shown in the lower two frames of Fig. 2, is now nearly independent of the number of smoothing runs carried out for $\text{NSMTK} \geq 15$.

The third smoothing procedure attempted involves the fitting of a quintic polynomial to a moving group of nine data points using the modified least squares technique of Savitzky and Golay.^{10,15} The resulting first differential is found to be very nearly identical to the lowest curve of Fig. 2.

DISCUSSION

The first differential of our IE function (Fig. 2) reveals sharp, reproducible (to better than 30 meV) fine structure superimposed on a steplike background function extending between 12.1 and 13.4 eV. Such fine structure is expected to arise through autoionization of highly excited Rydberg levels of neutral Xe, each process resulting in a feature on the direct IE function which is a reflection of the electron impact excitation function relating to the appropriate neutral Xe^* state.

A discussion of the theoretical and experimental line profiles of neutral autoionizing states manifesting themselves on IE curves has been given by Bolduc and Marmet.¹⁷ The form of excitation function will, of course, be dependent on whether or not the transition $(np, ml) \text{Xe}^* - \text{Xe}^* ({}^2P_{1/2}) + e^-$ is optically allowed or not. The excitation function for optically forbidden transitions (e.g., parity forbidden $s-p'$ transitions in the present case) is expected to be sharply peaked at threshold, whereas optically allowed transitions (e.g., $s-s'$, $s-d'$, ...) are expected²² to possess excitation functions rising much less steeply with energy. Since some excitation functions sharply "peak" near threshold,²² it is not surprising that we observe the first differential of the Xe^+ IE function (Fig. 2) minimize below zero twice and approach zero at a number of other energies. The correlation between the energies of our minima and the various Rydberg levels converging on the $\text{Xe}^* ({}^2P_{1/2})$ limit is seen to be very good (Table I).

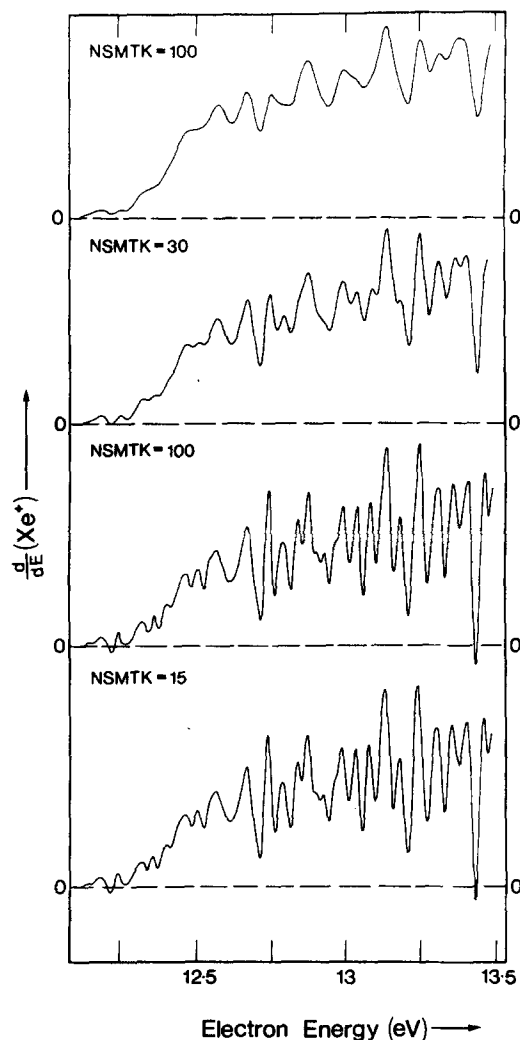


FIG. 2. The first differential of the ionization efficiency function of xenon. The top two frames show results of simple five-point moving averages smoothing. The lower two frames show results of weighted five-point moving averages smoothing. The lowest frame also shows the result of modified least squares smoothing (see text). NSMTK = number of smoothing runs performed on raw data.

TABLE I. Rydberg levels of Xe converging on $\text{Xe}^+ {}^2P_{1/2}$.

| s' | p' | d' | f' | Observed (± 0.03 eV) |
|------------|------------------------|------------------------|------------|------------------------------|
| | | | | 12.23 |
| | $n=7$ | | | |
| | 12.25 (1) ^a | | | |
| | 12.28 (2, 1) | | | 12.28 |
| | 12.31 (0) | | | |
| | | $n=6$ | | 12.35 |
| | | 12.34 (2) ^a | | 12.39 |
| | | 12.37 (3) | | 12.44 |
| | | 12.46 (1) | | 12.49 |
| $n=8$ | | | $n=4$ | 12.54 |
| 12.58 | | | 12.58 | 12.62 |
| | $n=8$ | | | |
| | 12.73 (1) | | | |
| | 12.75 (2, 1) | | | 12.72 |
| | 12.76 (0) | | | |
| | | $n=7$ | | |
| | | 12.77 (2, 3) | | 12.77 |
| | | 12.83 (1) | | 12.82 |
| $n=9$ | | | $n=5$ | 12.87 |
| 12.89 | | | 12.89 | 12.92 |
| | $n=9$ | $n=8$ | | |
| | 12.98 | 12.99 (2, 3) | | 12.95 |
| | | 13.02 (1) | | 13.01 |
| $n=10$ | | | $n=6$ | |
| 13.06 | | | 13.05 | 13.06 |
| $n=11$ | $n=10$ | $n=9$ | $n=7$ | |
| 13.16 | 13.10 | 13.12 (2, 3) | 13.16 | 13.15 |
| | | 13.14 (1) | | |
| $n=12$ | $n=11$ | $n=10$ | $n=8$ | |
| 13.22 | 13.19 | 13.21 | 13.22 | 13.21 |
| $n=13$ | $n=12$ | $n=11$ | $n=9$ | |
| 13.27 | 13.25 | 13.26 | 13.27 | 13.27 |
| $n=14$ | $n=13$ | $n=12$ | $n=10$ | |
| 13.30 | 13.29 | 13.29 | 13.30 | |
| $n=15$ | $n=14$ | $n=13$ | $n=11$ | |
| 13.33 | 13.31 | 13.32 | 13.33 | 13.33 |
| $n=18$ | $n=18$ | $n=18$ | $n=18$ | |
| 13.37 | 13.37 | 13.38 | 13.40 | 13.38 |
| $n=\infty$ | $n=\infty$ | $n=\infty$ | $n=\infty$ | |
| 13.44 | 13.44 | 13.44 | 13.44 | 13.43 |
| | | | | 13.48 |

^a J values are shown in brackets.

The energies of the Rydberg states tabulated in Table I are from the experiments of Stebbings and co-workers^{3,4} and the very recent measurements of Grandin and Husson.¹ Energies of Rydberg states not detected in the above-mentioned experiments have been deduced from the Rydberg formula:

$$E = E_{\infty} - R/(n - \mu)^2,$$

where the quantum defect μ has been taken from Moore¹⁸ for optically allowed levels. In the case of optically forbidden transitions, it has been assumed that μ varies

slowly with the principle quantum number n and that for a given series $\mu(s, p, d, \dots) \approx \mu(s', p', d', \dots)$, where s, p, d, \dots are Rydberg levels converging on $\text{Xe}^+ ({}^2P_{3/2})$ and the primes indicate levels converging on $\text{Xe}^+ ({}^2P_{1/2})$. Though it is not possible to unambiguously assign all observed minima to specific Rydberg levels, it appears that some of the detected structure is almost certainly attributable to parity-forbidden transitions of $s-p'$ type (e.g., at 12.28 and 12.72 eV).

Due to differences in energy resolution and sensitivity, a detailed comparison of our results with earlier data is not feasible; however, comparison in terms of the number of minima observed and the general shape of the various first differential curves shows that our curve compares rather well with the relatively much lower resolution RPD one obtained by Grasso,⁶ who detected 14 clear minima compared to our 24. Both sets of data reveal a very pronounced minimum at the $\text{Xe}^+ ({}^2P_{1/2})$ onset. The data of Johnson *et al.*¹⁶ and Hashizume and Wasada² also provide some evidence for this particular minimum.

Our present data confirm earlier observations^{6,16} of a relatively sharp increase in Xe^+ flux at the ${}^2P_{1/2}$ ionization potential, contrary to the findings of Marmet and co-workers,⁵ whose filtered IE function revealed six shallow structures and showed little evidence of any sharp variation in the vicinity of the ${}^2P_{1/2}$ threshold. Moreover, three of the processes reported by these authors (at 12.30, 12.67, and 12.92 eV) were attributed to formation of temporary Xe^- states, on the grounds that interpretation in forms of optically forbidden p' levels could be ruled out owing to inconsistent quantum defects. Available data appear to contradict this interpretation. The photoexcitation results of Grandin and Husson,¹ as well as those of Rundel *et al.*³ have resolved fine structure splitting in some np' autoionizing levels and, using their data, we calculate the quantum defects for np' ($J=1$) levels to be 3.62, 3.59, 3.59, and 3.63 for $n=7, 8, 9$, and 10, respectively; corresponding quantum defects for np' ($J=0$) levels are 3.53 and 3.53 for $n=7$ and 8. For larger values of n , J splitting becomes too small to be of consequence here.

It is of interest to note that our data shows clear structure above the $\text{Xe}^+ ({}^2P_{1/2})$ onset. There is evidence for this in all previous studies on Xe, except in the data of Marmet and co-workers.⁵ A short-lived Xe^- state is probably involved here; however, it must be mentioned that although weak Xe^- resonant states have been observed in highly sensitive electron transmission studies in the energy range 18–20 eV,^{19,20} none have yet been detected in the 12–14 eV range.

CONCLUSIONS

IE functions for Xe have revealed sharp fine structure in the energy range between $\text{Xe}^+ ({}^2P_{3/2})$ and $\text{Xe}^+ ({}^2P_{1/2})$ limits. Comparison of the energies corresponding to minima in the IE first differential with the known positions of Xe Rydberg states converging on the ${}^2P_{1/2}$ limit gives good agreement and strongly suggests that some parity-forbidden transitions of the type $s-p'$ are being

observed. Comparison of present data with earlier recent work indicates reasonable agreement in terms of gross features, except in one case.⁵ Present data also confirm earlier indications that the Xe^+ flux increases sharply above the $^2P_{1/2}$ onset; it is therefore not necessary to invoke a "competition between states" hypothesis,⁵ whereby it has been suggested that the cross section for ionization to the Xe^+ ($^2P_{1/2}$) state proceeds at the expense of that via the $^2P_{3/2}$ channel.

Earlier assignment⁵ of some of the observed structure to Xe^- resonances may have been based on grounds which did not consider that fine structure splitting of np' Rydberg levels of Xe can be quite considerable for low values of n and, consequently, calculations of quantum defects with weighted means of J values may lead to false conclusions.

ACKNOWLEDGMENTS

It is a pleasure to thank Professor Allan Maccoll for laboratory facilities and constant encouragement during the course of these and similar experiments and Professors D.W.O. Heddle and J. B. Hasted for most useful discussions. One of us (D.C.F.) wishes to express appreciation to University College, London, for warm hospitality. D. M. is grateful to the Science Research Council for financial support.

¹J.-P. Grandin and X. Husson, *J. Phys. B* **14**, 433 (1981).

- ²A. Hashizume and N. Wasada, *Int. J. Mass Spectrom. Ion Phys.* **36**, 291 (1980).
- ³R. D. Rundel, F. B. Dunning, H. C. Goldwire, Jr., and R. F. Stebbings, *J. Opt. Soc. Am.* **65**, 628 (1975).
- ⁴R. F. Stebbings, C. J. Latimer, W. P. West, F. B. Dunning, and T. B. Cook, *Phys. Rev. A* **12**, 1453 (1975).
- ⁵P. Marmet, E. Bolduc, and J. J. Quemener, *J. Chem. Phys.* **56**, 3463 (1972); P. Marmet, *J. Chem. Phys.* **63**, 249 (1975).
- ⁶F. Grasso, *Int. J. Mass Spectrom. Ion Phys.* **2**, 357 (1969).
- ⁷R. E. Huffman, Y. Tanaka, and J. C. Larrabee, *Appl. Opt.* **2**, 927 (1963); *J. Chem. Phys.* **39**, 902 (1962).
- ⁸H. M. Rosenstock, K. Draxl, B. W. Steiner, and J. T. Herron, *J. Phys. Chem. Ref. Data* **6**, Suppl. 1 (1977).
- ⁹K. Maeda, G. P. Semeluk, and F. P. Lossing, *Int. J. Mass Spectrom. Ion Phys.* **1**, 395 (1968).
- ¹⁰D. Mathur, *J. Phys. B* **13**, 4703 (1980).
- ¹¹A. Maccoll and D. Mathur, *Org. Mass Spectrom.* (in press).
- ¹²D. Mathur, *Chem. Phys. Lett.* (in press).
- ¹³H. H. Arsenault and P. Marmet, *Rev. Sci. Instrum.* **48**, 512 (1977).
- ¹⁴C. Lanczos, *Applied Analysis* (Pitman, London, 1957).
- ¹⁵A. Savitzky and M. J. E. Golay, *Anal. Chem.* **36**, 1627 (1964).
- ¹⁶C. P. Johnson, J. D. Morrison, and A. L. Wahrhaftig, *Int. J. Mass Spectrom. Ion Phys.* **26**, 1 (1978).
- ¹⁷E. Bolduc and P. Marmet, *Can. J. Phys.* **51**, 2108 (1973).
- ¹⁸C. E. Moore, *Atomic Energy Levels*, Natl. Bur. Stand. Circ. 467, 1953.
- ¹⁹L. Sanche and G. J. Schulz, *Phys. Rev. A* **5**, 1672 (1972).
- ²⁰D. Mathur (unpublished data).
- ²¹I. H. Suzuki and K. Maeda, *Mass Spectrosc. (Tokyo)* **27**, 31 (1979).
- ²²D. W. O. Heddle, *Contemp. Phys.* **17**, 443 (1976).